

# VNIR-SWIR using OreXpress spectroradiometer as a spectral approximation method to differentiate epithermal mineralization alteration phases. A case study from Jacinto and Big Golden Hill, Cuba

Virginia González-Acosta<sup>1\*</sup> , Víctor M. Velasco-Herrera<sup>1</sup> , Emmanuel Zúñiga<sup>2</sup> , Willie Soon<sup>3</sup>, Enrique C. Piñero-Pérez<sup>4,5</sup> , Higinio Pimentel-Olivera<sup>4,6</sup> and Eligio Eymil-Romero<sup>4,7</sup>

## Abstract

Spectral differences (range: 350-2500 nm) between the three alteration phases related to low and high sulfidation epithermal mineralization has been studied in the Jacinto deposit (Beatriz, Sur de Elena, and El Limon Nuevo veins) and the Big Golden Hill sector, respectively, located in the Cuban Cretaceous volcanic, Camagüey and Las Tunas provinces. This study has revealed the following differences between the phases: (a) Phase I: associated with the lithological type of quartz with massive and/or brecciated texture, where gold mineralization develops. At 600-800 nm, the signals identified responds with goethite and at 1400, 1900 y 2200 nm, as montmorillonite and nontronite. The reflectance value is 30 -50%, although in the El Limón Nuevo vein is 30-40%. (b) Phase II: Related to the argillic alteration zone composed by sericitic or silicified quartz and ferrous minerals such as limonite and hematite. It only occurs in Beatriz and Sur de Elena veins. At 600-800 nm, the signal is associated with ferrous minerals and at 1400, 1900, and 2200 nm, to clays minerals as montmorillonite, halloysite, and nontronite. The reflectance value is 30 – 50%. The difference between both Phases is in the amplitude and shape of the absorption feature at 1400 nm. (c) Phase III: it is located near the volcanic rock, composed by illite-smectite-quartz, without gold content and nearby to propylitic zone. At 600-800 nm, the feature indicates the presence of goethite and at 1400, 1900, and 2200 nm, to montmorillonite, illite, and nontronite. The reflectance value is 30 - 40%. The Big Golden Hill sector is characterized by peaks related to goethite and nontronite at 600-800 nm and pyrophyllite at 1400, 1950 and 2165 nm, typical of advanced argillic alteration. The reflectance value reaches 55%. This study represents one of the first applications of reflectance spectroscopic techniques in Cuban mineral deposits.

**Key words:** VNIR-SWIR, OreXpress, epithermal mineralization, low sulfidation, high sulfidation, Cuba.

## Resumen

Se han estudiado las diferencias espectrales (intervalos 350 - 2500 nm) entre las tres fases de alteración vinculadas con la mineralización epitermal de baja y alta sulfuración en el depósito Jacinto (vetas Beatriz, Sur de Elena y El Limón Nuevo) y el sector Big Golden Hill, respectivamente, localizados dentro del arco volcánico cretácico de Cuba, provincia de Camagüey y Las Tunas. El estudio ha revelado las siguientes diferencias: (a) Fase I: se asocia al tipo litológico de cuarzo con textura masiva y/o brechosa y mineralización aurífera. A 600-800 nm, la señal identificada responde con goetita y a 1400, 1900 y 2200 nm, a la montmorillonita y nontronita. El valor de reflectancia es de 30- 50%, aunque para El Limón nuevo es de 30-40%; (b) Fase II: relacionada con la zona de alteración argílica, compuesta por cuarzo sericitico o silicificado y minerales ferrosos como la limonita y hematita. Esta fase solo ocurre en Beatriz y Sur de Elena. A 600-800 nm, la señal corresponde a minerales ferrosos y a 1400, 1900 y 2200 nm con los arcillosos como la montmorillonita, halloysita y nontronita. El valor de reflectancia es de 30 - 50%. Las diferencias entre ambas fases radican en la amplitud y forma del rasgo de absorción en 1400 nm; (c) Fase III: se ubica próxima a la roca volcánica, compuesta por illita-esmectita-cuarzo, sin contenido de oro y cercana a la zona propilítica. En 600-800 nm el rasgo indica la presencia de goetita y a 1400, 1900 y 2200 nm, a montmorillonita, illita y nontronita. El valor de reflectancia es de 30- 40%. El sector Big Golden Hill se caracteriza por picos relacionados a goethita y nontronita a 600 - 800 nm y a pirofilita a 1400, 1950 y 2165 nm, propio de alteración argílica avanzada. El valor de reflectancia alcanza los 55%. Este trabajo representa una de las primeras aplicaciones de técnicas espectroscópicas de reflectancia en depósitos de Cuba.

**Palabras clave:** VNIR-SWIR, OreXpress, mineralización epitermal, baja sulfuración, alta sulfuración, Cuba.

Received: June 26, 2023; Accepted: May 24, 2024; Published on-line: July 1, 2024.

Editorial responsibility: Dra. Ruth Esther Villanueva-Estrada

\* Corresponding author: Virginia González Acosta, [vga6902@gmail.com](mailto:vga6902@gmail.com)

<sup>1</sup> Instituto de Geofísica, Universidad Nacional Autónoma de México, Circuito Exterior, C.U., Coyoacán, CDMX, 04510, México. [vmv@igeofisica.unam.mx](mailto:vmv@igeofisica.unam.mx)

<sup>2</sup> CONAHCYT-Instituto de Geografía, Universidad Nacional Autónoma de México, Circuito Exterior, C.U., Coyoacán, CDMX, 04510, México. [ezuniga@geografia.unam.mx](mailto:ezuniga@geografia.unam.mx)

<sup>3</sup> Institute of Earth Physics and Space Science (EPSS), 04510, Sopron, Hungary and Center for Environmental Research and Earth Sciences (CERES), Salem, Massachusetts 01970, USA.

<sup>4</sup> Empresa Geomínera de Camagüey, Camagüey, Cuba. <sup>5</sup> [enriquepp@geocmg.minem.cu](mailto:enriquepp@geocmg.minem.cu), <sup>6</sup> [higiniopo@geocmg.minem.cu](mailto:higiniopo@geocmg.minem.cu) and <sup>7</sup> [eligioer@geocmg.minem.cu](mailto:eligioer@geocmg.minem.cu)

Virginia González-Acosta, Víctor M. Velasco-Herrera, Emmanuel Zúñiga, Willie Soon, Enrique C. Piñero-Pérez, Higinio Pimentel-Olivera, Eligio Eymil-Romero

<https://doi.org/10.22201/igeof.2954436xe.2024.63.3.1721>

## 1. Introduction

Cuba has a variety of metallic and industrial mineral occurrences throughout the national territory belonging to different geological conditions and environments. One of the perspectives for gold mineralization and base metals is found in the region of the Cretaceous Volcanic Arcs (CVA), which it extends from the east of the province of Ciego de Ávila to the boundaries of Las Tunas province. Studies carried out in this region since the first half of the 20th century have revealed several mineral areas prospects that have been exploited only in small areas. The first ones took place during the neocolonial epoch (1902-1958), with the exploitation of alluvial gold (López *et al.*, 2017), until more recently, when the area of interest has gained a higher mineral value.

Subsequent and continuous geological researchers have had as their main objective to be the search for mineralized zones and the increase of the geological knowledge. This is because this region standouts as one of the most perspective areas for the search of favorable zones of gold mineralization and other metals (Czhestakanova, 1966; Shevchenko *et al.*, 1979; Ovchinikov *et al.*, 1981; Tchounev *et al.*, 1981; Iturralde-Vinent *et al.*, 1986; Durañona *et al.*, 1990; Capote *et al.*, 1991; Piñero *et al.*, 1992; Pimentel *et al.*, 1992, 1993; Capote, 1999; Capote *et al.*, 2002, 2005; Donet *et al.*, 2014; Cazañas *et al.*, 2014).

In the region of the CVA, different mineral deposits of diverse genesis are developed, such as: La Unión porphyry Au-Cu deposit (exploration by Mineral Siboney Goldfields-Geominera S.A. from 1994 to 1996, Alonso *et al.*, 2001, Ulloa *et al.*, 2011), Jacinto and Golden Hill (GH) mineral (field Figure 1, epithermal origin with low and high sulfidation, respectively). These were selected in the present research as study area because they are economically the most important for gold mineralization into the CVA region (Ovchinikov *et al.*, 1981; Tchounev *et al.*, 1981; Iturralde-Vinent *et al.*, 1986; Durañona *et al.*, 1990; Pimentel *et al.*, 1992, 1993, 2018; Meeling, 1996; Simon *et al.*, 1999; Kesler *et al.*, 2004; Piñero *et al.*, 2008, 2011, 2021).

Besides, in other countries several investigations using VNIR/SWIR (visible to near infrared / short-wave infrared) reflectance spectroscopy techniques have proven to be very useful for the rapid identification of hydrothermal alteration minerals (Thompson *et al.*, 1999) for mineral exploration.

Since the creation of the various spectral libraries (usgs\_min, jpl\_lib, jhu\_lib, igcp\_lib, etc.), diverse software such as: ENVI, ERDAS, Spec\_minTM, and others, are also useful for mineral discrimination based on their absorption features in different wavelength positions (Grove *et al.*, 1992, Clark *et al.*, 1993). Many authors have used these tools for various purposes Thomp-

son *et al.*, (1999), Ducart *et al.*, (2006), Simpson, (2015), Arbiol and Lyne (2021), Wang *et al.*, 2021, Zhou *et al.*, 2022, Zhou *et al.*, 2023, and others.

Jacinto deposit is a vein system (Figure 2) where Beatriz, Sur de Elena and El Limón Nuevo veins are the most prospective (Piñero *et al.*, 2021). GH mineral deposit comprises three sectors (Figure 3), where Three Hill (TH) and Little Golden Hill (LGH) sectors are exploited. Big Golden Hill (BGH) sector is not yet exploited but there is a high degree of knowledge in its geological exploration phase (Pimentel *et al.*, 2018).

The study area extends from Camagüey to Las Tunas provinces, territories belonging to the central-eastern region of Cuba (Figure 1). It is located approximately 29 km east of the City of Camagüey and reaches to 8 km to the east of the city of Las Tunas. The main access is through the central highway of Cuba, from which there are other secondary roads crossing it. The most important urban centers located within the area are Cascorro, Sibanicú, Amancio Rodríguez, Jobabo, Gúaimaro, Najasa, Colombia and the already mentioned city of Las Tunas.

Due to the economic importance of the study area, the main objective and contribution of this research is to deepen on the knowledge of the region and to apply of spectral pattern analysis as a preliminary method of approximation to differentiate, from spectral pattern, between phases of alteration in both deposits in Cuba. Spectroscopic measurements techniques have not been applied before for these purposes either in the study areas or in the Cuban national territory.

In Cuba, the use of remote sensing techniques, as an efficient way of capturing information for the study of altered mineral zones, has not been widely explored, so the present research seeks to provide, a step forward into a methodological way for its the knowledge, management, and application and to be effectively introduced into the geological investigation.

### 1.1 Study areas

#### 1.1.1 Jacinto deposit

The Jacinto deposit is developed in the form of stockwork of a vein system, which are named as Beatriz, Beatriz NW, Sur de Elena, Elena, El Limón Nuevo, La Ceiba, El Limón Viejo, Franklin, La Esperanza, TE-33 and La Naranja (Figure 2). The Beatriz, Sur de Elena and El Limón Nuevo veins were the most studied localities and the focus in this work (Piñero *et al.*, 2011, 2021). The Beatriz and Sur de Elena veins are located about 2.5 km southeast of Loma Jacinto and cover an area of 0.715 km<sup>2</sup> (71.5 ha). El Limón Nuevo vein is about 2.5 km SE of Loma Jacinto and covers about 0.115 km<sup>2</sup> (11.5 ha). (Piñero *et al.*, 2021).

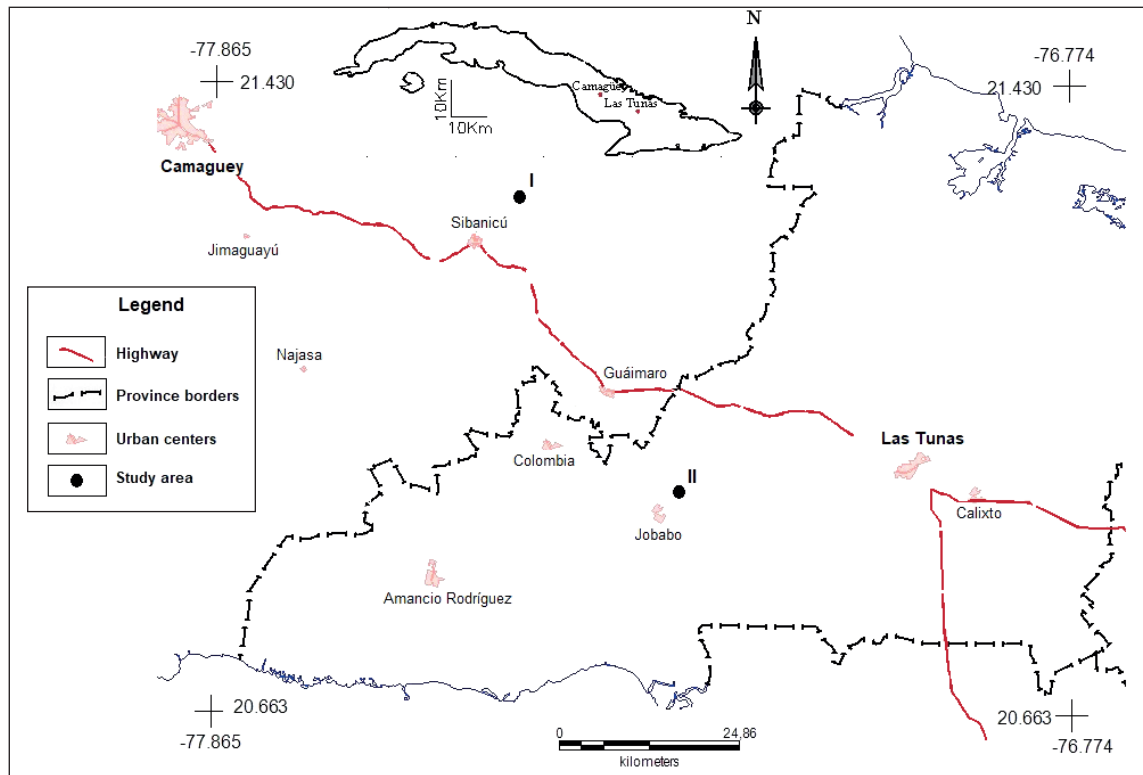


**Figure 1.** Location map of the study area. I- Jacinto deposit, II- Big Golden Hill sector.

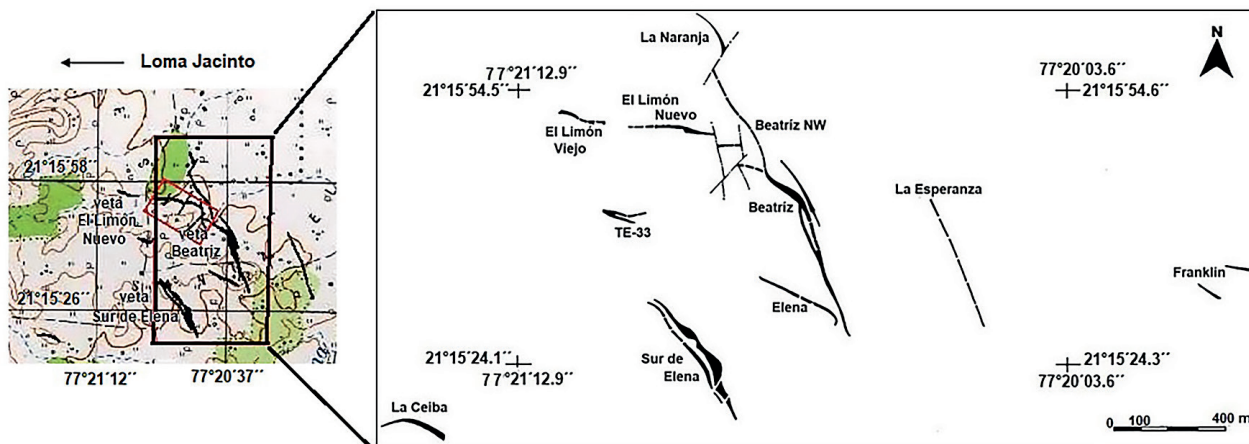


**Figure 2.** Scheme of distribution of the veins in the Jacinto deposit (modified from Simon *et al.*, 1999; Kesler *et al.*, 2004 and Piñero *et al.*, 2011). The coordinate system used was GEODETIC WGS-84.

### 1.1.2 Big Golden Hill sector

The Big Golden Hill sector is an exploitation concession and one of the three main sectors of the GH mineral field, together with LGH and TH (Figure 3). It is located 8 km NE of the town of Jobabo and occupies an area of 0.08 km<sup>2</sup> (8.0 ha). (Pimentel *et al.*, 2018).

### 1.2 Geological setting of the Camagüey – Las Tunas

Two structural levels are recognized - the folded substrate or Caribbean Plate (CARIB) and the neoautochthonous or cover terrain (Iturralde-Vinent, 1996). The first of these is exposed through the CVA and the sedimentary deposits of the Late Campanian-Maastrichtian-Upper Eocene that overlay it. The



**Figure 3.** A-Location map of the GH mineral field and its three sectors. B- View of an outcropped area in the BGH sector. The coordinate system used was GEODETIC WGS-84.

predominant mineralization in the CVA is epithermal occurring in various levels of the volcano-sedimentary column. The lithological units, linked to epithermal mineralization, are Crucero Contramaestre Formation (cct k2 - k5-1) in the case of Golden Hill and Camujiro (cjo k1-2) and La Sierra Formation (ls k2) to Jacinto deposit (Iturralde-Vinent *et al.*, 1986; Piñero *et al.*, 1992; Kesler *et al.*, 1994; Simon *et al.*, 1999). It is characterized by a great lithological variety in both the plutonic and volcanic-sedimentary complexes with ages ranging from the Lower Cretaceous (Neocomian) to the Upper Cretaceous (Campanian). It was described by four phases of magmatism, according to their petrographic, petrochemical, spatial and temporal distribution (granosienitic, granodioritic, plagiogranitic and alkaline leucocratic granites (Maraguan granites) complex, being the first three the most important and less important the last one (Pérez and Sukar 1994).

### 1.3 Geological characteristics

#### 1.3.1 Jacinto deposit

It has been classified as a low sulfidation deposit (LS) of the Au-Ag adularia – sericite type (Simon *et al.*, 1999). Gold is present in the native form and occurs in quartz associated to its crystalline structure. The silver contents are negligible.

Piñero *et al.*, 2021 describe the layer texture in samples from the Jacinto veins. Their study allowed them to differentiate between five main stages, separated by brecciation. Stage I contains gold, and it is composed of microcrystalline to finely granular quartz with a massive or brecciated texture. Stage II contains gold, and it is composed of layers of microcrystalline to finely granular quartz and adularia, alternating with layers of microcrystalline to coarsely granular quartz. Stage III contains gold, and it is characterized by layers of calcite and microcrystalline

or finely granular quartz in a stratified or massive texture. Stage IV is sterile in gold, and it is composed of microcrystalline to coarsely granular quartz, with less calcite and adularia. Stage V is composed of massive calcite.

The key minerals of the proximal alteration zones are sericite, quartz and pyrite cut by adularia and quartz. The gangue minerals are calcite, adularia, and gypsum in smaller quantities.

The Jacinto deposit is hosted by the Camujiro and La Sierra Formations (Figure 4). The Camujiro Formation (cjo k1-2 - Upper Cretaceous, Cenomanian and Upper Cretaceous, Turonian) is constituted by volcanic breccias, lavas, clastic lavas, tuffs and agglomerative tuffs; all of them display a variable composition, with dominant alkaline and calc-alkaline rocks; lavas from trachybasalt and shoshonites to trachyandesites, sandy and detritic limestones (de Huelbes and Bernal, 2013).

The rocks of the Camujiro Formation are propylitized and tectonic, forming green-colored breccias, without mineralization. These serve as host rocks to quartz veins with a predominant brecciated texture and, to a lesser extent, massive texture, with low-sulfidation epithermal gold mineralization of the adularia-sericite type.

In the north-northwest portion of the sector, the La Sierra Formation (ls k2 - Upper Cretaceous, Campanian) appears, consisting of lavas and lava breccias with K-alkaline rhyolitic, rhodacytic, and dacitic composition (de Huelbes and Bernal, 2013). In altered (argillitized) sections, these appear as cutting bodies with a northwest direction.

Piñero *et al.*, (2021), suggests that these intrusions have created conditions or conduits for Jacinto hydrothermal system. The hydrothermal alterations have affected the rocks of the Camujiro Formation, giving rise to zones of argillic and propylitic alteration, which may be associated with epithermal vein systems of precious metals, as observed in the case of Jacinto.

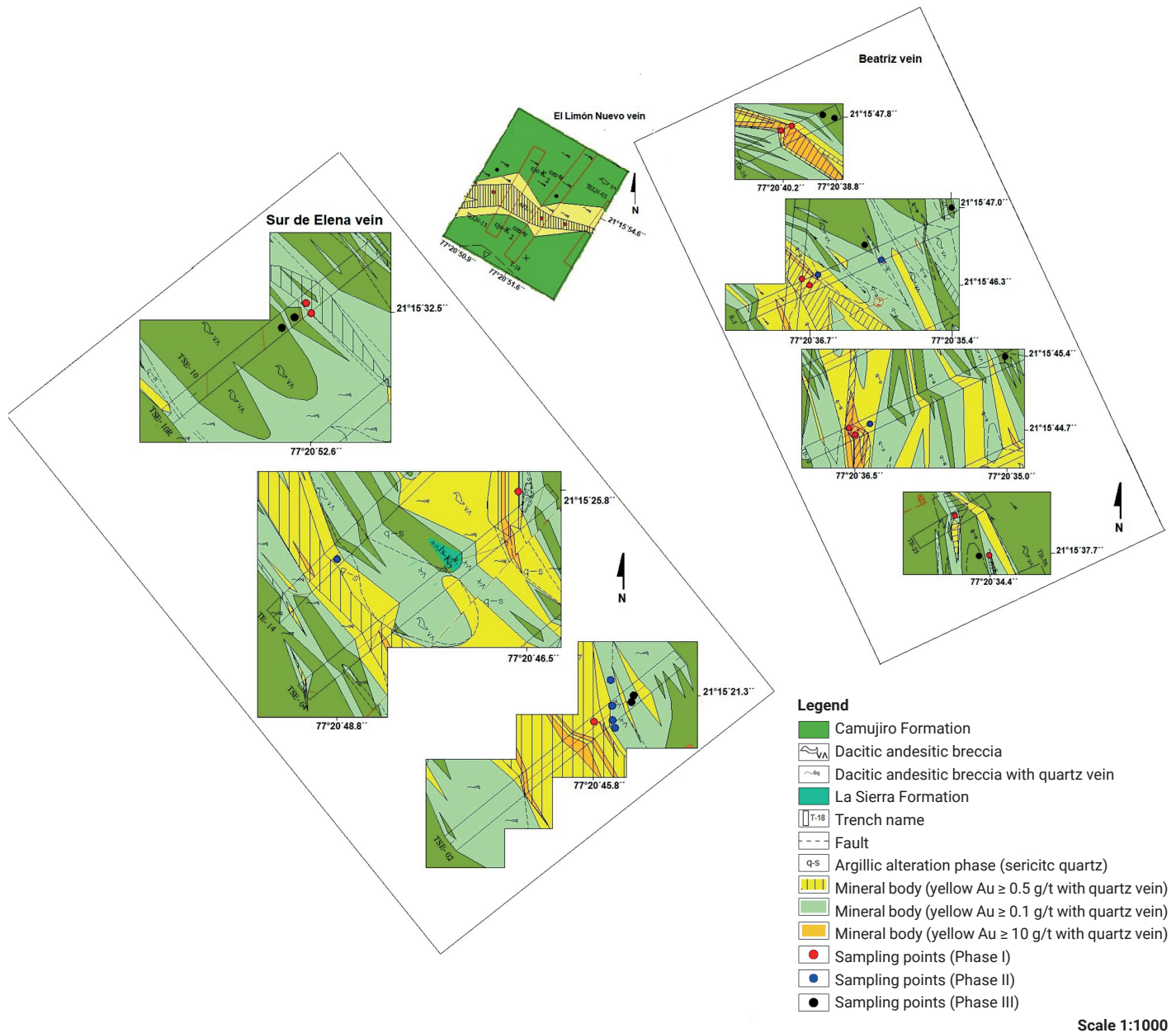


**Figure 4.** Geological map and sections of the sampling locations of Jacinto deposit (El Limón Nuevo, Beatriz, and Sur de Elena veins) (modified from Piñero *et al.*, 2011, 2021). The coordinate system used was GEODETIC WGS-84. The location of the samples is shown in the Table 1.

Regarding the host rocks, hydrothermal alterations have affected the rocks of the Camujiro Formation, giving rise to quartz-sericite and propylitic alteration zones, which are associated with the veins under study. Piñero *et al.*, (2008, 2011, 2021) determined from petrographic studies of thin sections and mineralogical analyses that the host rock contains sericite, quartz, and pyrite, cut by adularia and quartz near the veins. Additionally, another assemblage is represented by illite-sericite-quartz, without pyrite. Outside the illite-sericite zone, there are propylitic assemblages in which plagioclase has altered to chlorite, albite, and calcite, and amphibole and pyroxene have altered to chlorite.

Piñero *et al.*, (2021) determined that the main indicators and criteria for mineralization include outcrops of the mineralization (quartz with brecciated and massive textures, sometimes banded) (Stage I) and alteration zones characterized by the presence of sericite, quartz, and pyrite. The illite-sericite assemblage is followed by propylitic assemblages.

Piñero *et al.*, (2008, 2021) describe that the mineralization process in the Jacinto deposit is divided into two phases: endogenous, in which magnetite is first associated with the host rocks, and then the epithermal mineralization begins to play part where pyrite, chalcopyrite, sphalerite, galena, gold and tetrahedrite

**Table 1.** Jacinto deposit. Geographic coordinates of the sample rocks.

Veins	Number of samples	Latitude N	Longitude W	
<b>Beatriz</b>				
Phase I	B-1 (TB-16*)	21°15'47.8''	77°20'39.2''	
	B-1a (TB-16*)	21°15'47.7''	77°20'39.2''	
	B-5	21°15'46.3''	77°20'36.7''	
	B-5a (R-5*)	21°15'46.4''	77°20'36.8''	
	B-8a (TB-12 sup*)	21°15'44.8''	77°20'36.5''	
	B-9a	21°15'44.7''	77°20'36.5''	
	B-13 (TE-23 sup*)	21°15'37.7''	77°20'33.4''	
	B-14 (TE-23 trench*)	21°15'38.0''	77°20'33.7''	
	Phase II	B-6	21°15'46.4''	77°20'36.6''
		B-6a (R-5*)	21°15'46.5''	77°20'36.0''
B-8b (TB-12 sup*)		21°15'44.8''	77°20'36.3''	
Phase III	B-2 (TB-16*)	21°15'47.8''	77°20'38.9''	
	B-3a (TB-16*)	21°15'47.8''	77°20'38.8''	
	B-7 (R-5*)	21°15'46.7''	77°20'36.2''	
	B-7a (R-5*)	21°15'47.0''	77°20'35.4''	
	B-9-1	21°15'45.4''	77°20'35.0''	
B-12	21°15'37.6''	77°20'33.5''		
<b>Sur de Elena</b>				
Phase I	SE-5 (TSE-02*)	21°15'23.0''	77°20'45.7''	
	SE-7 (TSE-04*)	21°15'25.8''	77°20'46.5''	
	SE-8a (TSE-10*)	21°15'32.4''	77°20'52.5''	
	SE-9ab (TSE-10*)	21°15'32.5''	77°20'52.6''	
Phase II	SE-4	21°15'23.3''	77°20'45.6''	
	SE-6 (TE-14*)	21°15'24.0''	77°20'48.8''	
	SE-3a (TSE-02*)	21°15'21.3''	77°20'46.4''	
	SE-3b (TSE-02*)	21°15'23.0''	77°20'45.6''	
	SE-3c (TSE-02*)	21°15'23.0''	77°20'45.6''	
Phase III	SE-1 (TSE-02*)	21°15'21.3''	77°20'46.4''	
	SE-2	21°15'21.3''	77°20'46.4''	
	SE-8c (TSE-10*)	21°15'32.3''	77°20'52.8''	
	SE-9c	21°15'30.5''	77°20'53.5''	
<b>El Limon Nuevo</b>				
Phase I	ELN-10	21°15'54.4''	77°20'51.6''	
	ELN-10a	21°15'54.1''	77°20'51.3''	
	ELN-10a-1	21°15'54.1''	77°0'50.9''	
Phase III	ELN-11a	21°15'54.6''	77°20'51.6''	
	ELN-1a-1	21°15'54.4''	77°20'50.9''	

appear. The second phase is hypergenic and is represented by goethite and hematite and other iron oxides and hydroxides.

Previous petrographic analyses (Piñero *et al.*, 2008, 2011) described areas with predominant minerals of propylitic alteration, such as quartz, carbonate, sericite, chlorite, epidote. In thin sections, the adularia potassium feldspar appeared, thus corroborating the interpretation of Simón *et al.*, (1999) concerning deposits of epithermal low sulfidation with adularia.

### 1.3.1.1 Beatriz vein

Beatriz vein in the center of the Jacinto deposit (Figure 2), with a course development of approximately 600 meters. It develops from the center from where a branching occurs that gives rise to three veins (A, B and C), linked to three mineralized zones of the same name, and characterized by quartz + intense silicification + calcite, accompanied by alteration zones argillic quartz-sericitic-kaolinitic, limonitization and hematitization, with oxidized and leached sulfides. The gold content may also appear associated with a gray to whitish gray breccia that forms from a silicified and tectonized part of the sericitic quartz rock, closely related to the quartz vein.

Piñero *et al.*, (2021) in mineralogical studies showed that the phases were maintaining crystalline and amorphous quartz, plagioclase, chlorite, sodium and potassium feldspar, the adularia crystalline phase, pyroxene, micas, calcite, Fe oxides, pyrite and chalcopyrite, and clays (as Montmorillonite + Illite and Chlorite + Montmorillonite). Gold is associated with quartz of > 0.03 mm in size. Previous results of Scanning Electron Microscopy indicate that the dimensions of the particles can reach an average value of 5.1  $\mu$ .

An initial macroscopically description revealed that the mineralization is associated with the stage I, describe previously. Surface samples are taken close to the trenches made in the vein.

### 1.3.1.2 Sur de Elena vein

Piñero *et al.*, (2021), indicated that the vein is in an undulating relief approximately 500 meters SW of the Beatriz vein and heading parallel to it and it is composed of white to gray quartz and calcite. The vein is highly tectonized and limonitized, accompanied by a quartz-sericitic-kaolinitic alteration zone, limonitized and hematized, with oxidized and leached sulfides.

The vein reaches its greatest development as a vein and mineral zone towards the central part. It has an irregular shape, its widest part is in the southeast, then it branches into two that continue intermittently to the northwest. Similar characteristics of geological structure and mineralization are observed throughout the vein.

Gold mineralization could link to quartz + calcite veins with breccia and/or massive texture accompanied by zones of argillic alteration (quartz - sericitic - kaolinitic?) limonitized and hematized. The mineralization carrier is also the gray breccia forming from the silicified and tectonized quartz-sericitic rock, with few sulfides.

A first inspection of material revealed the presence of silicified, hematized quartz, sericitic quartz veins, breccia texture, calcite may appear. The vein appears in a trench and outcrops in surface. Towards the ends, appear the volcanic rock that extends to the outermost part of the vein and belongs to the propylitic alteration.

### 1.3.1.3 El Limón Nuevo vein

The center of the vein is delimited by the TE-18 trench (Piñero *et al.*, 2011), located at a slight elevation, to the W of the Beatriz vein (Figure 2). It is composed by a vein of white quartz where gold can also appear associated with a gray to whitish-grey breccia that forms from a sericitic quartz rock, in parts silicified and tectonized, with up to 5% of sulfides, in close relationship with the quartz vein, belonging to stage I. It belongs to the Camujiro Formation. The mineral accumulation has a length of 260 m. The rocks are propylitized and tectonized, forming green colored breccia, without mineralization and of broad development.

An initial revision of samples revealed the presence of white quartz with large clasts of gray vulcanites, almost perfect breccia texture and massive texture. The vein is found in trench and outcrops at the surface. Vulcanites appear at the ends of the vein.

## 1.3.2 Big Golden Hill sector

The Golden Hill mineral field is classified as high sulfidation (HS) pyrite-enargite type. The gold mineralization is associated with the advanced argillic hydrothermal alteration phase. The primary ore is massive and scattered sulfides, pyritic, overlaid by the oxidized ores. (Pimentel *et al.*, 2018).

The element association indicates hypogenic (Au-Cu) and supergenic (Au-Ag) features. The hydrothermal alteration phase is associated with the vesicular quartz and quartz-alunite facies in the center-west of the area, to the quartz-pyrophyllitic facies in the southeast, which are enveloped by argillic alteration and this in turn by propylitic. The key metallic minerals in the hypogenic phase includes pyrite, enargite, chalcocite, with Au disseminated within pyritic ore, whereas in the supergenic phase appears native Au. The key minerals in the proximal alteration include quartz, kaolinite, alunite, pyrophyllite, and diaspore, where the gangue minerals are hypogenic (quartz, kaolinite, alunite, pyrophyllite,

and diaspore) or supergenic (hematite, goethite, jarosite, and quartz) specimens.

The BGH sector (Figure 5) belong to the Crucero-Contra-maestre Formation (cct k2-k51- Upper Cretaceous, Turonian and Upper Cretaceous, Lower Campanian), that consists of tefroid sandstones, conglomerates, gravelites, tuffs, limolitic tufites, silicified limestones, gray silicites, lavobreccias, andesites, basalts, and basalt-andesites (de Huelbes and Bernal, 2013).

## 2. Materials and Methods

As it was before mentioned, the main objective of this work has been to carry out the spectral differentiation and characterization of the main alteration zones or phases of mineral deposits using a portable spectroradiometer or VNIR-SWIR. This is an internationally well-known technique applied in Cuba for the first time. The materials used as well as the methodology conducted are as described below. The research scheme was divided into three stages (Figure 6).

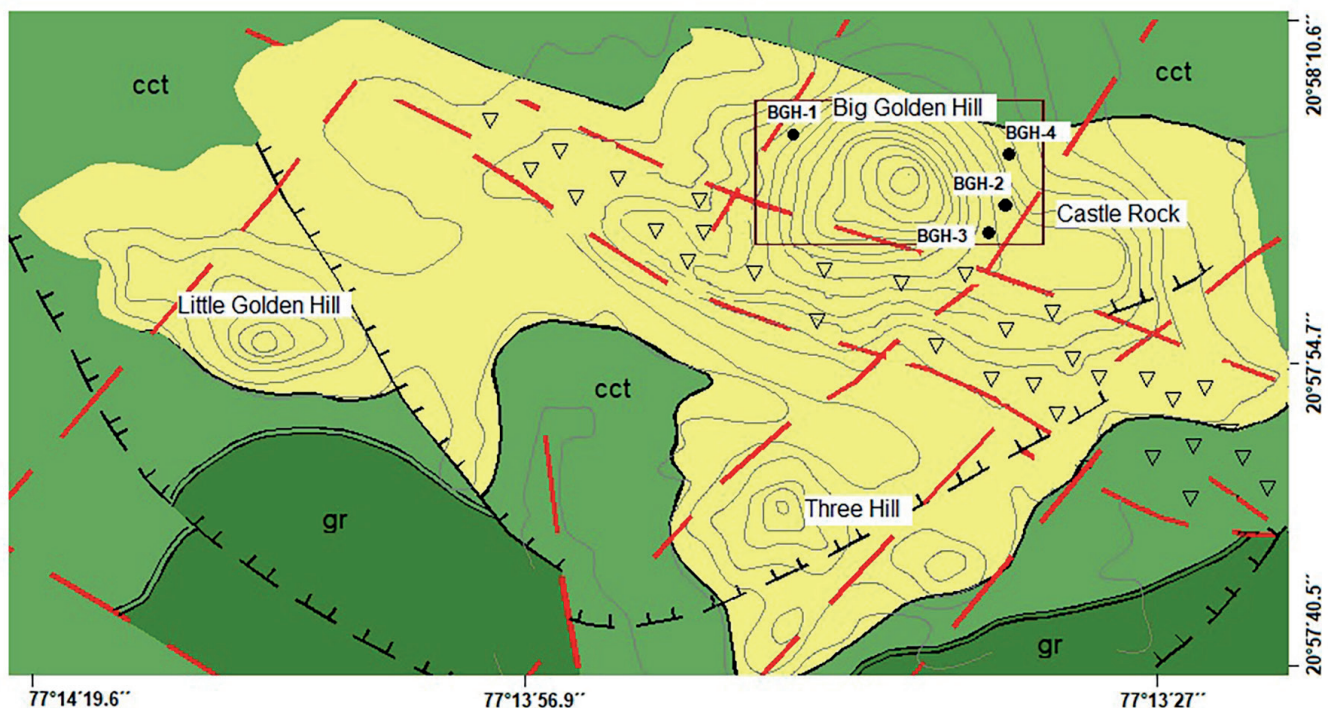
*Stage I: Data preparation.* Geological and topographic sheets at a scale of 1:100,000 (Institute of Geology and Paleontology (IGP), 2015) and previous geological information described in geological reports of both deposits (IGP, ONRM, Empresa

Geominera Camagüey) were revised and compiled into a database, in order to select the fieldwork itineraries and sampling points. These were established according to previous geological information and prior meetings and consultation with specialist colleagues related to the study areas with a previous geological exploration work in these mineral deposits.

*Stage II: Description and data collection.* A detailed geological description about rock types and alteration phases, (Figures 4 and 5) from the wall of the trench into the veins and photographs of the outcrops were the data collected during the fieldwork. Samples collected in Cuba were analyzed at the laboratory in the Institute of Geophysics, UNAM, for petrographic, and chemical analysis. However, XRD analysis were not possible to be carried out due to the start of the pandemic. The minerals identified using OreXpress (OXps) for each alteration phase, were correlated to those described by Piñero *et al.*, 2008, 2011, 2021, and Pimentel *et al.*, 2018.

Table 3 shows the total number of samples taken during the fieldwork for each alteration phase which allowed to differentiate the position of the absorption features into the electromagnetic spectrum.

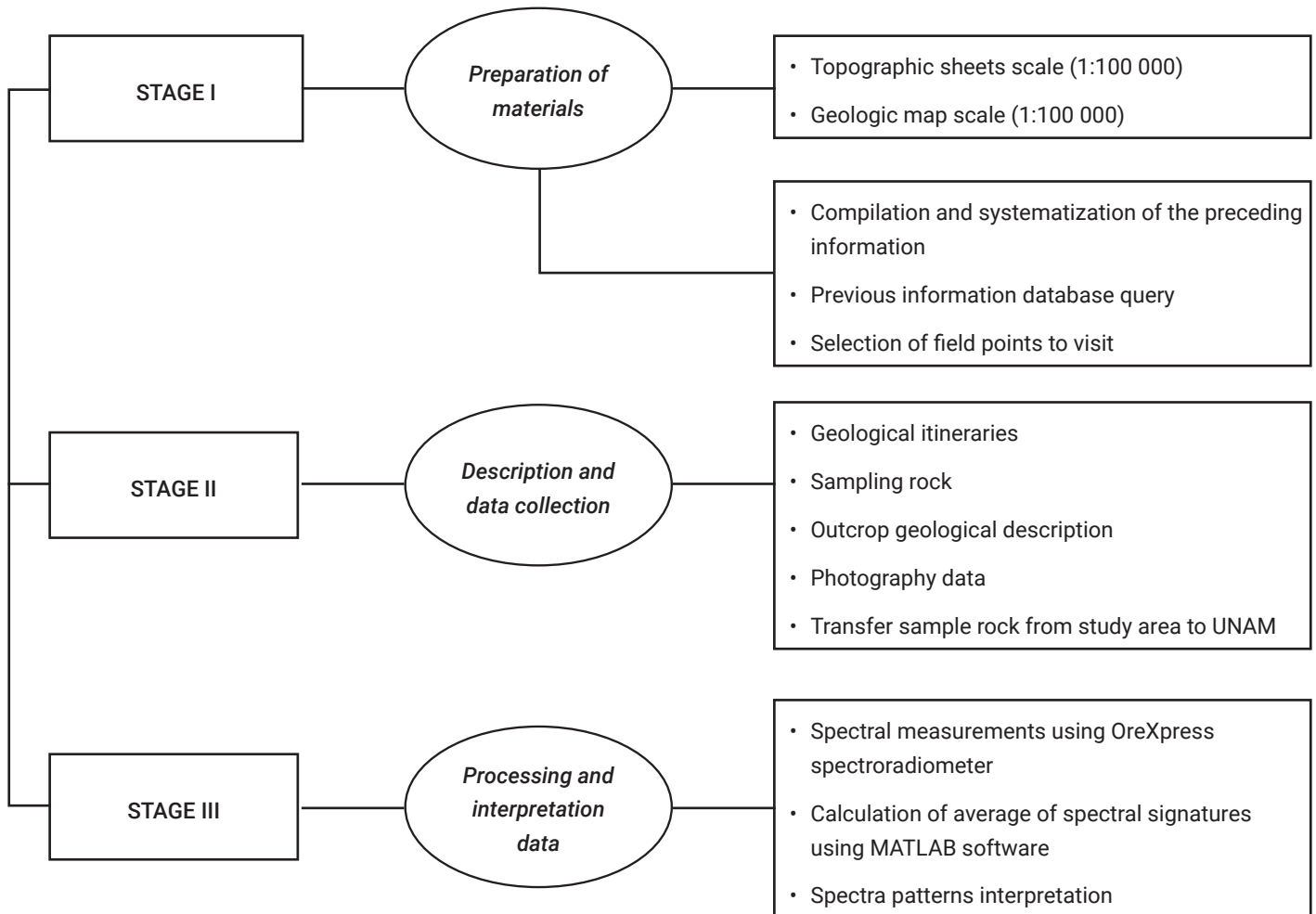
*Stage III: Data processing and interpretation.* Spectral measurements using OXps portable spectroradiometer were carried out at the Laboratorio de Petrografía y Microtermometría



**Figure 5.** Geological map and sampling locations of BGH sector. (modified Pimentel *et al.* 2018). The Coordinate system used was GEO-DETTIC WGS-84, red box: BGH sector study area, black dot: sampling points, dashed red lines: faults, cct: Crucero-Contra-maestre Formation, gr: Guaimaro Formation, light yellow color: Golden Hill mineral field limits: inverted triangle: alunite zone, dashed black lines with perpendicular black lines: circular structure Golden Hill. The location of the samples is shown in Table 2.

**Table 2.** Big Golden Hill sector. Geographic coordinates of the sample rocks.

Number of samples	Latitude	Longitude
BGH-1	20° 58' 03.2''	77° 13' 44.6''
BGH-2	20° 57' 58.4''	77° 13' 44.6''
BGH-3	20° 57' 57.9''	77° 13' 32.8''
BGH-4	20° 58' 01.8''	77° 13' 29.0''

**Figure 6.** Research flowchart.

(Laboratory of Petrography and Microthermics), belonging to the Departamento de Recursos Naturales (Department for Natural Resources) of the Instituto de Geofísica, Universidad Nacional Autónoma de México (UNAM), directly using the natural day-light and environment conditions.

With OXps portable spectroradiometer, model SM-500, was used to obtain the spectral evolution of each sample. The equipment measures wavelengths in a range from 350 to 2500 nanometers

in the full range of the electromagnetic spectrum. Some technical features of the OXps portable spectrometer are shown in Table 4 (<https://spectralevolution.com/products/hardware/field-portable-spectrometers-for-mining/orexpress/>). Samples were analyzed from the freshest and least weathered side. An average of 5 measurements were made per each sample, according to the different lithological or hydrothermal alteration phase type, in order to cover the entire area and to make it as representative as possible.

**Table 3.** Technical features of the OXps portable spectrometer.

Deposit	Sector	Alteration phases	Number of samples
Jacinto	Beatriz vein (B)	Phase I	8
		Phase II	3
		Phase III	6
	Sur de Elena (SE)	Phase I	4
		Phase II	5
		Phase III	4
El Limón Nuevo (ELN)	Phase I	3	
	Phase III	2	
BGH			4
<b>Total of samples</b>			<b>39</b>

**Table 4.** Minerals identified with the OXps spectroradiometer according to alteration phases.

Technic specifications	
Spectral range	350–2500nanometers
Spectral resolution	3nanometers (350-1000nanometers) 9nanometers @1500nanometers 6.5nanometers @2100nanometers
Spectral sampling bandwidth	1.5 nanometers (350-1000nanometers) 3.8nanometers @1500nanometers 2.5nanometers @2100nanometers
Wavelength reproducibility	0.1 nanometers
Wavelength accuracy	±0.5 bandwidth

## 2.1 Equipment calibration

Once the equipment was turned on, the DARwinSP with a USGS database incorporated for the interpretation of the spectra software activated. After the machine-equipment connection activated, a window opened and through Bluetooth the EZ software-ID opened. To start the spectral measurements, it is important to calibrate the equipment. For doing this, the position of the head on the Spectralon plate (white reference), must be on a clean surface. After the measurement, its spectrum appears on the screen, and the equipment calibrates to begin the measurements.

## 2.2 Spectral measurements

The calibration window is switched to the target. The head is placed in the position of the angle to be measured in the direction of the sample and the signal is executed on the monitor. Measured spectrum is shown on the monitor and on the right side appears its reflectance value and wavelength. The information is included into a file X.sed, and it is opened in a software like

ENVI, Specmin\_home, and so on, to work with it. Additionally, copying the wavelength and reflectance values to a spreadsheet and plotting the spectra is also possible.

## 2.3 Matching with EZ-ID software

Once this software opened and the sample measured, two spectra signatures are offered. One belongs to the sample (blue color) and the other to the USGS software library (red color) with the percentage of the mineral correlation between them (from a maximum to a minimum values), as well as a list of minerals to which it could correspond and that begins with the highest association ( $\geq 90\%$ ), depending on the absorption features present at different position of wavelengths, in the short infrared region, mainly due to alteration minerals. This window also shows the place of origin from where the samples are taken from which their spectrum was established as a reference into the library.

The final spectrum that identifies each of the hydrothermal alteration phases per deposit (Figure 7) is defined from the average of the measurements belonging to each hydrothermal alter-

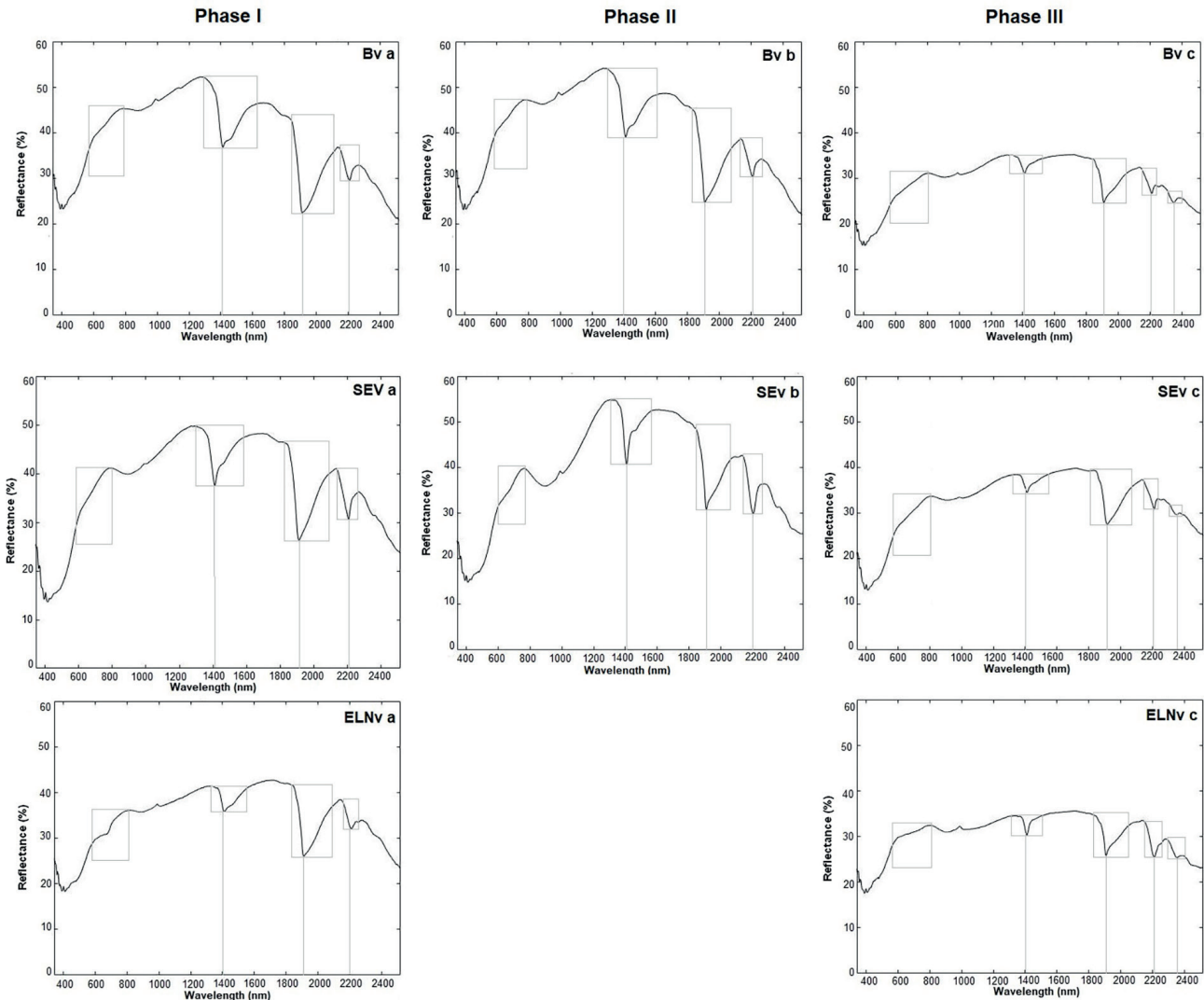


**Figure 7.** It shows the spectral features of the alteration phases present in the veins of the Jacinto deposit. Phase I is represented by the letter a. Phase II by b, and Phase III by c. Bv indicates the Beatriz vein, SEv the Sur de Elena vein, and ELNv the El Limon Nuevo vein.

ation phase. It is considered that the association grade between the spectrum of the mineral, obtained from the measurements with the spectroradiometer, and that reported in the spectral library database was  $\geq 90\%$ . The calculation process has been carried out for 195 measurements using the MATLAB software (R2019a-student license). The spectra patterns interpretation has contemplated a visual analysis considering the shape and depth of the absorption features and the reflectance value.

### 3. Results and Discussion

Through the processing and interpretation of spectral information, the three main alteration zones or phases, previously identified by Piñero *et al.*, 2008, 2011, 2021, based on geological

exploration research carried out in the Jacinto deposit, could be well differentiated. Additionally, the advanced argillic alteration phase for the BGH sector was reaffirmed according to the spectral data too, with the presence of minerals characterizing it, such as pyrophyllite, as it was also described by Pimentel *et al.*, 2018. The description of these alteration phases or zones is provided below.

Figures 7 and 8 show the light gray boxes with dashed lines corresponding to the average absorption positions performed with the OXps on the samples along the entire spectrum. The boxes at the 1400, 1900 and 2200 nanometer wavelength position represent the absorption features, which are attributed to the presence of clay minerals, such as: montmorillonite, nontronite. That position is the most distinctive pattern to differentiate the hydrothermal alteration phases considering its shape and width.

### 3.1 Jacinto deposit

It is characterized by the presence of three main hydrothermal alteration phases or zones (Figure 7). A detailed description of the spectral signature that allows to differentiate and characterize each alteration phase are shown in Table 6 and Figure 11.

(a) *Phase I* - Associated with the lithological type of quartz with massive and/or brecciated textura, named as Stage I from Piñero *et al.*, 2021. Results are shown in Figure 7 (represented by the letter a). In this phase, four absorption features along the spectral signatures are present in all veins. The spectral signature in the visible region between 600 – 800 nanometers is represented by the presence of goethite as an iron hydroxide as described by Piñero *et al.*, 2021. This pattern is less represented into the ELN vein. A distinctive feature in all veins occurs at 1400, 1900 and 2200 nanometers, which responds to the presence of clay minerals, such as: montmorillonite, nontronite which belong to smectite group, identified in Table 5, although the shape and depth of peak is different (box with gray continuous line). The reflectance value in this position is less than 30 % from the lower part of the absorption feature at 1900 nanometers, until 50 % although in the ELN vein. This pattern was very different, which allowed to differentiate among the rest of the veins, with values from near to 30% to 40%.

(b) *Phase II* – There is an alteration zone with the presence of quartz-sericite or silicified, limonitized, and hematitized, linked to the argillic alteration phase, where the main minerals characterizing it are kaolinite, montmorillonite, smectite (<https://www.ugr.es/~minechil/apartado14.htm>). Results are shown in Figure 7 (represented by the letter b). This phase does not occur into the ELN v. Four absorption features are present in the Bv and Sev, along the spectral signatures in the wavelength range. The spectral signature in the visible region between 600 – 800 nanometers is represented by the presence of goethite and limonite as an iron oxide and hydroxide. A distinctive feature occurs at 1400, 1900 and 2200 nanometers, which results from the presence of clay minerals, mainly by the montmorillonite

as representative mineral in argillic alteration phase, beside of halloysite and may be nontronite which belong to smectite group, identified in Table 5. The reflectance value in this position is nearly 30 %, until more than 50 %.

It is important to emphasize that the difference between this phase and the previous one is evident at 1400 nanometers, where the amplitude and shape of the absorption feature at that position are illustrated in Figure 7.

(c) *Phase III* - Alteration zone proximal to the volcanic rock represented by the presence of illite-sericite-quartz assemblages, without gold content, near the propylitic alteration zone. Results are shown in Figure 7 (represented by the letter c). The spectra of this alteration phase are characterized by five absorption features along the wavelength range. The spectral signature in the visible region between 600 – 800 nanometers is represented by the presence of goethite as an iron hydroxide. A distinctive feature occurs at 1400, 1900 and 2200 nanometers, which respond to the presence of clay minerals such as montmorillonite, illite and nontronite which belong to smectite group, identified in Table 5. The most pronounced spectral feature occurs at 1900 nanometers. The reflectance value in this position is nearly 30 % at 1900 nanometers, until more than 40 %.

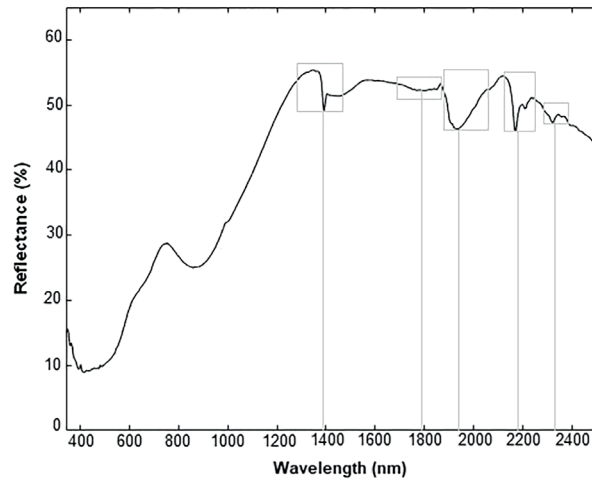
### 3.2 Big Golden Hill sector

Figure 8 shows the six absorption features in the wavelength ranges from 600 to 2320 nanometers. The signal observed in the range 600-750 nanometers defines the response for iron oxide and hydroxide minerals, characterized by the presence of goethite in the gossan. The maximum reflectance value is 55%. The value of the absorption features for this spectrum is reported in Table 6 and Figure 11.

Once the spectra for each vein and sector were obtained, specific to each phase of hydrothermal alteration, the next task was to establish those the minerals identified with the spectroradiometer characterizing each of the veins of the Jacinto deposit and the BGH sector.

**Table 5.** Type of mineralization and its relationship with the values of the absorption features.

Ore deposit	Minerals
<b>Jacinto</b>	
Phase I	Montmorillonite, heulandite, laumontite, nontronite, goethite
Phase II	Montmorillonite, goethite, laumontite, halloysite, nontronite, stilbite, limonite
Phase III	Montmorillonite, goethite, illite, rhodonite, nontronite
<b>Big Golden Hill sector</b>	Goethite, nontronite, pyrophyllite, anorthite



**Figure 8.** Spectral reflectance curve of samples from the Big Golden Hill sector.

**Table 6.** Type of mineralization and its relationship with the values of the absorption features.

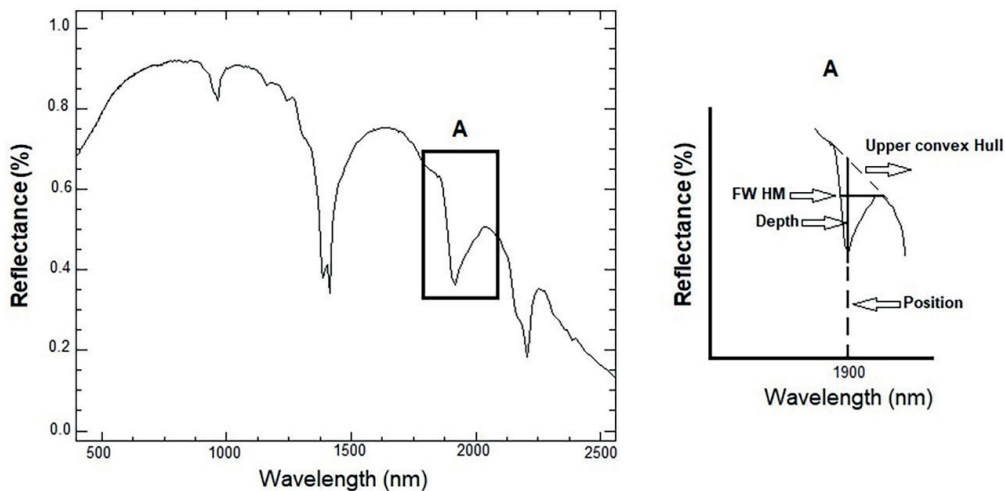
Hydrothermal alteration phases		Range of wavelength position versus depth (nanometers)				
<b>Jacinto (LS)</b>						
Phase I	600-800	1270-1650	1830-2150	2150-2260		
		1400	1900	2200		
Phase II	600-800	1300-1580	1840-2100	2130-2270		
		1400	1900	2200		
Phase III	600-800	1360-1545	1840-2110	2130-2240	2280-2370	
		1400	1900	2200	2340	
<b>Big Golden Hill (HS)</b>						
Oxidized zone	600-750	1360-1550	1730-1840	1870-2080	2120-2230	2270-2340
		1400	1900	2170	2200	2320

Table 5 shows a general description to all minerals identified with the OXps spectroradiometer for each hydrothermal alteration phase present in the different veins and the sector, respectively. These are in correspondence with the geological description in Piñero *et al.* (2008, 2011, 2021) which determined that the predominant minerals for the low sulfidation system were montmorillonite, stilbite, goethite, laumontite, halloysite, illite, rhodonite, nontronite, muscovite, and limonite.

Pimentel *et al.* (2018) described in the high sulfidation system that the minerals present were goethite, pyrophyllite, nontronite and, in a smaller proportion, Ca-rich plagioclase. Goethite has a marked representation in the visible region of the spectrum (Figure 8), typical for iron oxides - hydroxides. Pyrophyllite appears mixed with kaolinite, alunite, and quartz, which indicate a positive response as an alteration mineral, being associated with advanced argillic alteration to which the

gold mineralization is related. On the other hand, the presence of nontronite, which belongs to the smectites group minerals, could be an indicator of this, also typical for high sulfidation deposits. The results show the efficiency to apply this kind of technique for this purpose.

In Figure 9 an example of the feature analysis of an absorption peak (Thompson *et al.*, 1999) is displayed. Considering this principle, we proceeded to extract the wavelength range of each absorption signal in those spectra reported in Figures 7 and 8. The value of the amplitude of the absorption feature was determined empirically from a visual analysis of the spectrum, considering the Upper convex Hull and the position in the wavelength value (Figure 9). The rest of the parameters explained in Figure 9A, such as position and depth of the absorption features were considered after a differentiation between the different hydrothermal alteration phases in each deposit.



**Figure 9.** Example of spectrum curve. Detail A shows Hull’s feature, depth, position, and FWHM (adapted from Thompson *et al.*, 1999).

Once the position of the absorption features in the electromagnetic spectrum was obtained, we defined the Upper convex hull and Full Width Half- Maximum (FWHM) for each one. The upper convex Hull was calculated as an enveloping curve on the pixel spectra having no absorption features. Next, the Hull-quotient reflectance spectrum was derived by taking the ratio between the pixel reflectance spectrum and the enveloping upper convex Hull. These Hull quotient spectra were used to characterize absorption features, known to be attributed to a certain mineral of interest, in terms of their position, depth, width, asymmetry, and slope of the upper convex hull (van der Meer, 1995). The absorption band position ( $\lambda$ ) was defined as the band having the minimum reflectance value over the wavelength range of the absorption feature. The FWHM, in turn, was considered as the maximum width from one side to another into the absorption features.

Once the above mentioned parameters were defined, the next objective was to define the minimum and maximum range of the wavelength value of the absorption features into the spectrum. As reference, it was decided to take the Figure 10 from van der Meer *et al.*, (2012) where the author shows the main mineral deposit types in relation to their wavelength position of the absorption

feature related to the key alteration minerals. This figure was useful to corroborate if the position of the absorption features reported in Figure 10 are corresponded to those mentioned by the author as for low and high sulfidation mineralization and to validate the position obtained for each one.

According to van der Meer *et al.*, (2012), the identification of signals in the infrared visible regions is useful to infer the presence of transition metal ions (e.g., Fe, Cr, Co, Ni). These absorption peaks are related to atomic electronic transitions. The presence or absence of water and OH ion, carbonates and sulfates could be determined by absorption features in the short infrared region. On the other hand, the depth in the absorption band is related to the size of the grain as the amount of light scattered and absorbed by a grain is dependent on its size.

Using the information of Figure 10 as a guide, the minimum and maximum amplitude values of the absorption features for each of the hydrothermal alteration phases have been identified and evaluated.

Figure 11 illustrates the wavelength position for each absorption feature present in the spectra defined with the spectroradiometer according to alteration phase. We can summarize the characteristic absorption features according to the alteration

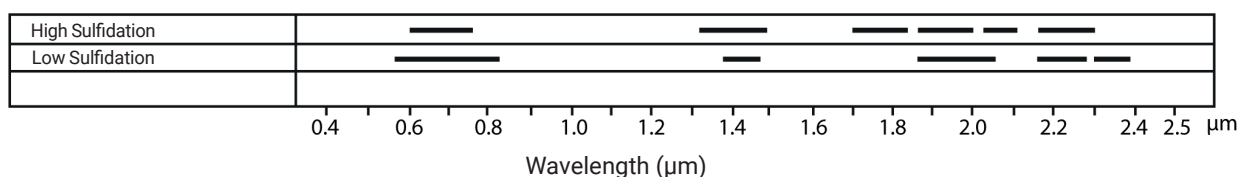


**Figure 10.** Types of epithermal deposits and their relationship with absorption areas (indicated in black lines) in the wavelength position, according to the spectrum of the alteration mineral.

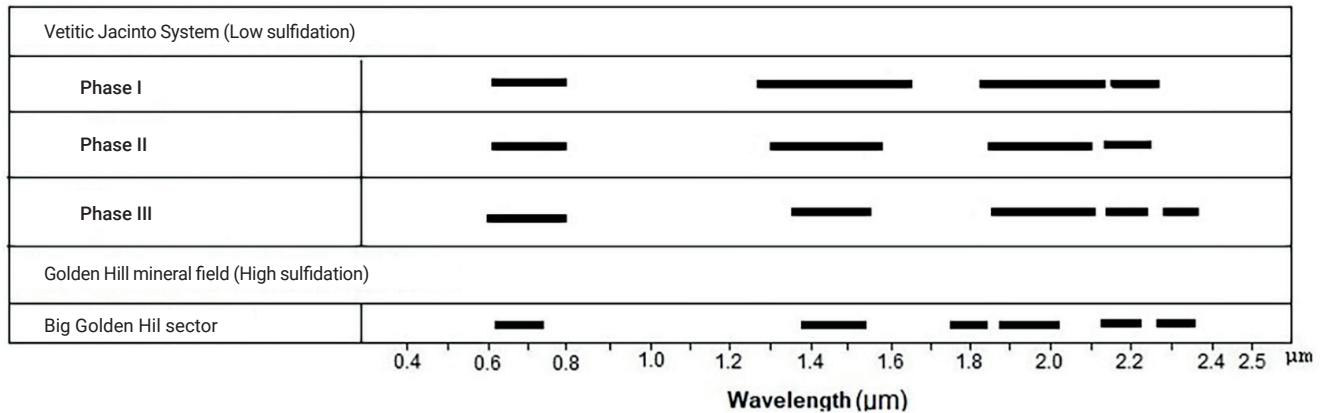


**Figure 11.** Absorption features defined according to the lithological type.

phases present in each mineral deposit. The following wavelength values in the spectrum, considering the amplitude and the position of the depth, are shown in Table 6. This classification allows to differentiate and define the proper wavelength positions for each alteration phase, where, in addition, they differ in reflectance values, although it is not the most important distinctive feature to consider.

Table 6 summarizes the information regarding the type of study mineralization linked to the position of the absorption feature that differentiate each of the alteration phases. The ranges of values indicate the maximum width that the absorption feature occupies, and the lower value is the position of the feature in its central value of wavelength.

The veins of the Jacinto deposit are separated by means of three alteration phases described previously. This one can be differentiated using the measured spectral characteristics.

The alteration phase I is characterized by four absorption features with wavelengths positioned in 600, 1400, 1900, and 2200 nanometers, respectively. Phase II is characterized also by four absorption features from the visible near infrared, like phase I, but the difference is in the shape, width and depth of the feature as shown in the Figure 7. The phase III is characterized by five absorption features from 1360 to 2370 nanometers. (Table 6).

The oxidized ore in the high sulfidation deposit is characterized by the presence of six absorption features (Table 6) at different wavelength positions ranging from the visible to the infrared, where a well-pronounced feature corresponding to the presence of iron oxides-hydroxides was observed. Those minerals of goethite identified were linked to very distinctive features in the near infrared where it is inferred that it is mainly related to pyrophyllite, which is typical of advanced argillic hydrothermal alteration phase. In addition, there are highly distinctive features in the near and short infrared compared to the other lithologies.

#### 4. Conclusions

Reflectance spectroscopy techniques, applied for the first time in Cuba, have allowed to differentiate and characterize different hydrothermal alteration phases linked to epithermal mineralization. Three alteration phases have been spectrally differentiated in the Jacinto deposit.

(a) *Phase I* – It is associated with the lithological type of quartz with massive and/or brecciated texture, where gold mineralization develops and is linked. It exhibits four absorption features. The feature at 600-800 nm is associated with the identified goethite mineral. The positions at 1400, 1900, and 2200 nm correspond to clay minerals identified as montmorillonite and nontronite, belonging to the smectite group. The reflectance value varies from under 30% at 1900 nm to a maximum of 50%. For the El Limón Nuevo vein, these fluctuate in the 30 to 40% range.

(b) *Phase II* – It is related to argillic alteration zone composed by sericitic or silicified quartz and ferrous minerals such as limonite and hematite. This phase only occurs the Beatriz and Sur de Elena veins. Four absorption features are distinguished. At 600-800 nm, it is associated with goethite and limonite. At 1400, 1900, and 2200 nm, clay minerals are linked. In this case, montmorillonite appears as the main mineral of the argillic alteration, along with others like halloysite and nontronite. The difference between Phase I and II lies in the amplitude and shape of the absorption feature at 1400 nm. The reflectance value ranges from around 30 to 50%.

(c) *Phase III* – It is an alteration zone near the volcanic rock, represented by illite-smectite-quartz arrangement, without gold content and close to the propylitic zone. Five absorption features are distinguished. The feature at 600-800 nm is associated with goethite. The positions at 1400, 1900, and 2200 nm correspond to clay minerals such as montmorillonite, illite, and nontronite.

The most pronounced feature is at 1900 nm. The reflectance values for all signals are around 30%, excepting for 1900 nm that reach 40%.

Alteration mineral arrangement of the Big Golden Hill sector is characterized by goethite and nontronite minerals, whose signals occur in the visible infrared region. In the rest of the spectrum have been detected absorptions linked to pyrophyllite, suggesting an advanced argillic alteration phase. The reflectance value reaches a maximum of 55%.

## 5. Acknowledgements

The authors wish to express their deepest gratitude to the different Mexican entities that guided and supported this work. Among them, the PCT Unit (Posgrado de Ciencias de la Tierra), UNAM, the Consejo Nacional de Ciencia y Tecnología (CONAHCYT), Mexico, for funding the research of which this article is a part. We offer thanks to Instituto de Geología y Paleontología / Servicio Geológico de Cuba and Empresa Geominera Camagüey for their support during the fieldwork stage. To colleagues, Domingo González Castellanos, Roberto Carlos Salas Nápoles, Luis Ramón Bernal Rodríguez, Daniel Torres Rodríguez, Manuel Soler, Jesús Manuel López Kramer, Augusto Antonio Rodríguez Díaz, Marcela Errasti Orozco, Irving Antonio González Romo, Ana Serra, María Teresa Rodríguez Coppola, for their unconditional help in carrying out the research. To Laboratorio de Petrografía y Microtermometría; Departamento de Recursos Naturales y Departamento de Radiación Solar, Instituto de Geofísica, UNAM. To Programa de Apoyo a los Estudios de Posgrado (PAEP), UNAM, for the financial support received. V.M. Velasco Herrera acknowledges the support from CONAHCYT-180148 grant and PAPIIT-DGAPA-UNAM IT102420. The authors also thank all the reviewers for their excellent comments.

## 6. Conflict of interest

The authors declare that they have no conflict of interest.

## 7. Data Availability Statement

The data underlying this article will be shared on reasonable request to the corresponding author.

## 8. References

- Alonso, J., Barroso, A., Molina, R., Valle, C., & Donet, P. (2001). *Informe Reconocimiento geológico para oro y otros metales en el sector Colombia-Barrueto, provincia de Camagüey*. Empresa Geominera Camagüey, Unpublished, Archivo del Instituto de Geología y Paleontología, La Habana, Cuba.
- Arboil C., & Layne G. D. (2021). Raman Spectroscopy Coupled with Reflectance Spectroscopy as a Tool for the Characterization of Key Hydrothermal Alteration Minerals in Epithermal Au–Ag Systems: Utility and Implications for Mineral Exploration. *Applied Spectroscopy*, 75(12) 1475–1496. doi: 10.1177/00037028211047869
- Capote, C. R. M., Santa Cruz, M. P., Díaz de Villalvilla, L. C., Brito, I., Pérez, M. R., Pereda, O., & González, E. (1991). *Proyecto temático-productivo (Thematic-productive project): Fundamentación del pronóstico y la búsqueda de minerales sólidos en la Región Siboney-Las Tunas*. Instituto de Geología y Paleontología y Empresa Geólogo-Minera Camagüey, Ministerio de la Industria Básica, Unpublished, Cuba.
- Capote, C. R. M. (1999). Análise do controle estrutural metalogénico em Cuba Centro-Oriental, com base em dados integrados. [Tese de doutoramento]. Universidad de Sao Paulo. Instituto de Geociencias Sao Paulo, Brazil.
- Capote, C. R. M., Santa Cruz, M. S., González, D. C., Altarriba, I., Bravo, F. P., De la Nuez, D. C. and Cazañas, X. D. (2002). *Evaluación del Potencial de Metales Preciosos y Base del Arco Cretácico en el Territorio Ciego-Camagüey-Tunas*. Informe Final del Proyecto I+D 224. Instituto de Geología y Paleontología, La Habana, Cuba.
- Capote, C. R. M., Santa Cruz, M. P., González, D. C., Díaz de Villalvilla, L., Peñalver, L., De la Nuez, D. C. & Santos, M. R. (2005). *Informe de la Tarea Generalización del Territorio Ciego-Camagüey-Las Tunas, Tema 7949, Mapa Geológico Digital de la República de Cuba, a escala 1:100000*. Instituto de Geología y Paleontología, La Habana, Cuba.
- Cazañas, X. D., Torres, J. L., Lavaut, W. C., Cobiella, J. L., Capote, C. R., González, V. A., & Figueroa, D. G. (2014). Mapa Metalogénico de la República de Cuba. [Mapa] 1:250 000. La Habana, Cuba: Instituto de Geología y Paleontología.
- Clark, R.N., Swayze, G. A., A.J. Gallagher, A. J., King, T. V. V., & Calvin, W. M. (1993). The U. S. Geological Survey, Digital Spectral Library: Version 1: 0.2 to 3.0 microns, U.S. *Geological Survey*, 93-592. 1340. doi: <https://doi.org/10.3133/ofr93592>
- Czhestakanova, V.C. (1966). *Informe de los trabajos de búsqueda y exploración realizados en los años 1964-1965, en los yacimientos auríferos de la zona de Guáimaro, en la provincia de Camagüey*. Instituto Cubano de Recursos Minerales. La Habana, Cuba.
- De Huelbes, J. A., & Bernal-Rodríguez L. R. (2013). *Léxico Estratigráfico de Cuba (3 ed.)* Instituto de Geología y Paleontología. La Habana, Cuba.
- Donet, P. C., Viltres, R. M., Barroso, A. & García, P. (2014). *Trabajo Temático Productivo Recopilación de la información, elaboración e interpretación Geológica existente de Oro en las provincias de Cama-*

- güey y Las Tunas. Empresa Geominera Camagüey, Cuba.
- Ducart, D. F., Crósta, A. P., Filho, C. R. S., & Coniglio J. (2006). Alteration Mineralogy at the Cerro La Mina Epithermal Prospect, Patagonia, Argentina: Field Mapping, Short-Wave Infrared Spectroscopy, and ASTER Images. *Economic Geology*, 101(5), 981-996. doi:10.2113/gsecongeo.101.5.981
- Durañona, D., Rodríguez, A., González, C. J. & Pimentel, H. O. (1990). *Informe final de prospección preliminar de polimetálicos en los sectores Guáimaro–Palo Seco*. Informe inédito
- Grove, C. I., Hook, S. J., & Paylor, E. D. (1992). *Laboratory reflectance spectra for 160 minerals 0.4 - 2.5 micrometers: JPL Publication 92-2, Jet. Propulsion Laboratory, Pasadena, CA.*
- Institute of Geology and Paleontology (2015). Geological sheets 1:100 000. La Habana, Cuba.
- Iturralde-Vinent, M.A., Thicke, U. & Piñero, E.C. (1986). *Informe final sobre el resultado del levantamiento geológico complejo y búsquedas acompañantes a escala 1:50 000 en el polígono CAME III. Camagüey 1981-1987*. Ministerio de la Industria Básica (current Ministerio de Energía y Minas). Oficina Nacional de Recursos Minerales.
- Kesler, S. E., Hall, C.M., Russell, N., Piñero E., Sánchez, R. C., Pérez, M. R. & Moreira, J. (2004). Age of the Camaguey Gold-Silver District, Cuba: Tectonic Evolution and Preservation of Epithermal Mineralization in Volcanic Arcs, *Economic Geology*, 99(5), 869-886. doi: <https://doi.org/10.2113/gsecongeo.99.5.869>
- López, J. M. K., Capote M. C.R., Rodríguez R.M., Alonso J.A., González C.D., Prieto C.C.M., López, O.C., de la Paz, M. D. & Boza M.D. (2017). Proyección estratégica de las investigaciones geológicas para oro en el archipiélago cubano. *Instituto de Geología y Paleontología*, Inédito La Habana, Cuba.
- Spectral Evolution. (s.a) Manual OreXpress-SM 500. Spectral Evolution. <https://spectralevolution.com/products/hardware/field-portable-spectrometers-for-mining/orexpress/>
- Universidad de Granada. (s.a) *Detalles de algunos tipos de alteración hidrotermal*. <https://www.ugr.es/~minechil/apartado14.htm>
- Melling, D. (1996). *Report of work for the 1995/1996 Period on the Golden Hill Exploration Area, Florencia-Jobabo Region, Republic of Cuba*. Macdonald Mines exploration LTD.
- Ovchinnikov, V., Balbis, C., Biriolin, V., Volcov, V., Bolotov, R. & Díaz, G.P. (1981). *Informe sobre los trabajos geológicos de búsqueda orientativa a escala 1:25 000 y detallada 1:10 000 para oro, cobre y molibdeno en la región Martí–Bartle–Las Tunas en los años 1976–1981*. Inédito.
- Pérez, M. R., & Sukar, K. (1994). *Magmatismo granitoideo cretácico en Camagüey*. Segundo Congreso Cubano de Geología, Santiago de Cuba.
- Pimentel, H. O. (1992). *Informe final sobre la verificación terrestre de anomalías aeromagnéticas en la región Guáimaro-Las Tunas*. Inédito, ONRM.
- Pimentel, H. O. (1993). *Informe de los trabajos de reconocimiento de anomalías magnéticas en el territorio Ciego-Camagüey-Tunas*. Empresa Geominera Camagüey, Cuba.
- Pimentel, H. O., Rodríguez F.E. & Sánchez. R.F. (2018). *Informe Final de la Exploración detallada de las menas oxidadas de Big Golden Hill*. Empresa Geominera Camagüey, Inédito, Camagüey, Cuba.
- Piñero, E. C. P., Rojas, R.C. & Iturralde-Vinent, M.A. (1992). *Informe sobre los resultados del levantamiento geológico complejo y búsquedas acompañantes a escala 1:50000 en el polígono CAME III. Camagüey, sector Loma Jacinto*. La Habana, Cuba, Oficina Nacional de Recursos Minerales.
- Piñero, E. C. P., Padrón, M.M., Mishekurina, E.Y. & Donet, P.C. (2008). *Exploración complementaria oro Jacinto, provincia Camagüey*. Proyecto. Empresa Geominera Camagüey, Inédito. Camagüey, Cuba.
- Piñero, E. C. P., Mishekurina, E.Y., Donet, P.C., Escobar, E.L.M., Rodríguez, F.E., Sánchez, R.F. & Pereira, A.F. (2011). *Exploración complementaria oro Jacinto veta El Limón Nuevo, provincia Camagüey. Informe final*. Empresa Geominera Camagüey, Inédito, Cuba.
- Piñero, E. C. P., Mishekurina, E., Rodríguez, A., Pereira, F. & Figueredo, M. (2021). *Exploración Complementaria Jacinto*. Empresa Geominera Camagüey.
- Simón G., Kesler, S.E., Russell, N., Halls, C.M., Bell, D N. & Piñero E.C. (1999). Epithermal Mineralization in an old Volcanic Arc: The Jacinto Deposit, Camaguey District, Cuba. *Economic Geology*, 94(4), 487-506. doi: <https://doi.org/10.2113/gsecongeo.94.4.487>
- Simpson, M. P. (2015). Reflectance spectrometry (SWIR) of alteration minerals surrounding the Favona epithermal vein, Waihi vein system, Hauraki Goldfield. *Proceedings of the Australasian Institute of Mining and Metallurgy New Zealand*, 409-418.
- Shevchenko, I., Frolov, V., Lugo, R., Dovnia, A., Laverov, Y., Burov, V. & Rob, J. (1979). *Informe sobre los trabajos de Levantamiento y Búsqueda a escala 1: 100 000 en las zonas de la parte Sur del Anticlinorio Camagüey. (Región Guáimaro-Victoria de Las Tunas)*. Oficina Nacional de Recursos Minerales, La Habana.
- Tchounef, D., Iturralde-Vinent, M. A. & Cabrera, R. (1981). *Geología del Territorio de Ciego- Camagüey-Las Tunas. Resultados de las investigaciones y del levantamiento geológico a escala 1:250 000*. Oficina Nacional de Recursos Minerales. Ministerio de Energía y Minas.
- Thompson, A. J. B., Hauff P. L. & Robitaille A. J. (1999). *Alteration mapping in Exploration: Application of Short-Wave Infrared (SWIR) Spectroscopy*. Reprint to from SEG Newsletter, 39(1), 16-27.
- Ulloa, M., M. S., Moura, M.A.; Boylho, N. F. & Olivo, G. (2011). The La Union Au Cu prospect, Camagüey District, Cuba: Fluid inclusion and stable isotope evidence for ore-forming processes, *Mineralium Deposita*, 46, 91-104. doi: <https://doi.org/10.1007/s00126-010-0313-8>
- Van der Meer, F. (1995). *Imaging spectrometry and the Ronda peridotites*. [PhD Thesis]. Wageningen.
- Van der Meer, F., van der Werff M. A. H., van Ruitenbeek J. A. F., Hecker A. C., Bakker H. W., Noomen F. M., van der Meijde M., Carranza M. J. E., de Smeeth B. J. & Woldai T. (2012). Multi- and hyperspectral geologic remote sensing: A review. *International Journal of Applied Earth observation and Geoinformation*, 14, 112-128. doi: <https://doi.org/10.1016/j.isprsar.2012.05.005>

[org/10.1016/j.jag.2011.08.002](https://doi.org/10.1016/j.jag.2011.08.002)

Wang, L., Percival, J., B., Hedenquist, J., W., Hattori, K., & Qin, K. (2021). Alteration Mineralogy of the Zhengguang Epithermal Au-Zn Deposit, Northeast China: Interpretation of Shortwave Infrared Analyses During Mineral Exploration and Assessment. *Economic Geology* 116(2), 389–406. doi: <https://doi.org/10.5382/econgeo.4792>

Zhou, Y., Wang, T., Fan, F., Chen, S., Guo, W., Xing, G., Sun, J., & Xiao, F. (2022). Advances on Exploration Indicators of Mineral VNIR-SWIR

Spectroscopy and Chemistry: A Review. *Minerals* 12(8), 958. doi: <https://doi.org/10.3390/min12080958>

Zhou, Y., Chen, Sh., Li, L., Fan, F., Zhang, H., Chen, J., Yang, K., Xiu, L., Xu, M., & Xing, G. (2023). Mapping hydrothermal alteration of the Au-Cu deposits in the Zhenghe magmatic-hydrothermal mineralization system, SE China, using Short Wavelength Infrared (SWIR) reflectance spectroscopy. *Journal of Geochemical Exploration*, 244, 107113. doi: <https://doi.org/10.1016/j.gexplo.2022.107113>